



## Original Article

The impact of probiotic *Clostridium butyricum* MIYAIRI 588 on murine gut metabolic alterations<sup>☆</sup>

Mao Hagihara<sup>a</sup>, Rieko Yamashita<sup>a</sup>, Asami Matsumoto<sup>a, b</sup>, Takeshi Mori<sup>b</sup>, Takayuki Inagaki<sup>d</sup>, Tsunemasa Nonogaki<sup>e</sup>, Yasutoshi Kuroki<sup>b, c</sup>, Seiya Higashi<sup>c</sup>, Kentaro Oka<sup>b, c</sup>, Motomichi Takahashi<sup>b, c</sup>, Hiroshige Mikamo<sup>b, \*</sup>

<sup>a</sup> Department of Molecular Epidemiology and Biomedical Sciences, Aichi Medical University, Japan

<sup>b</sup> Department of Clinical Infectious Diseases, Aichi Medical University, Japan

<sup>c</sup> Miyarisan Pharmaceutical Co., Ltd., Japan

<sup>d</sup> Department of Pharmacy, Nagoya University Hospital, Japan

<sup>e</sup> Department of Pharmacy, College of Pharmacy Kinjyo Gakuin University, Japan

## ARTICLE INFO

## Article history:

Received 9 December 2018

Received in revised form

24 January 2019

Accepted 11 February 2019

Available online 14 May 2019

## Keywords:

*Clostridium butyricum*

Microbiome

PICRUSt

Metabolic alterations

## ABSTRACT

**Introduction:** *Clostridium butyricum* MIYAIRI 588 (CBM 588) is a probiotic bacterium used in anti-diarrheal medicine in Japan. A few studies analyzed the changes in gut microbiome in patients treated with antimicrobials based on metagenomics sequencing. However, the impact of CBM 588 on gut metabolic alterations has not been fully elucidated. This study was to reveal the impact of CBM 588 on gut metabolic alterations.

**Material and methods:** In this *in vivo* study, mice were divided into four groups and CBM 588, clindamycin (CLDM), and normal saline (control) was orally administered (1. CLDM, 2. CBM 588, 3. CBM 588 + CLDM, 4. water) for 4 days. Fecal samples were collected to extract DNA for metagenomics analysis. Phylogenetic Investigation of Communities by Reconstruction of Unobserved States (PICRUSt) was used to obtain relative Kyoto Encyclopedia of Genes and Genomes (KEGG) pathway abundance information derived from metagenomics data.

**Results:** CLDM treatment resulted in a dramatic increase in Firmicutes phylum compared to non-CLDM-treated groups (control and CBM 588-treated group). Then, the CBM 588 + CLDM-treated group showed a trend similar in many metabolic pathways to the CLDM-treated group. On the other hand, the CBM 588 + CLDM-treated group showed higher relative abundance compared to the CLDM-treated group especially in starch and sucrose metabolism.

**Discussion:** We concluded that CBM 588 caused a gut microbiome functional shift toward increased carbohydrate metabolism. These results support the hypothesis that CBM 588 treatment modulates gut microbiome under dysbiosis conditions due to antimicrobials.

© 2019 Japanese Society of Chemotherapy and The Japanese Association for Infectious Diseases.

Published by Elsevier Ltd. All rights reserved.

## 1. Introduction

Microbial colonization of the gastrointestinal tract is a fundamental process in human life cycle [1,2]. Recent studies using 16S ribosomal RNA sequencing showed disease associations with dysbiosis or abnormal compositions of the gut microbiome [3–7].

Dysbiosis includes increase in bacterial numbers, decrease in bacterial biodiversity, and increase in abundance of the Proteobacteria and Firmicutes phyla [8–10]. Sequencing of 16S rRNA revealed alterations to taxonomic group and species composition in patients receiving antimicrobial therapy [11–13]. However, the metabolic activity and function of microbial communities are still unknown [5,14,15].

Antimicrobial treatments have been reported to be among the most powerful factors affecting the gut microbiome [11–13,15]. As a previous clinical study revealed, exposure to clindamycin (CLDM) resulted in the most pronounced and long-lasting change in gut

<sup>☆</sup> All authors meet the ICMJE authorship criteria.

\* Corresponding author. Department of Clinical Infectious Diseases, Aichi Medical University Hospital, 1-1 Yazakokarimata, Nagakute, Aichi 480-1195, Japan.

E-mail address: [mikamo@aichi-med-u.ac.jp](mailto:mikamo@aichi-med-u.ac.jp) (H. Mikamo).

microbial profiles [15]. The lincosamide CLDM has a broad spectrum of antimicrobial activity, including gram-positive aerobes and anaerobes and gram-negative anaerobes [16].

Probiotics are used with antimicrobials to prevent or cure diarrhea, and they are defined as live microorganisms that, administered in adequate amounts, confer a health benefit to the host [17]. They colonize the intestine and affect either microbiome composition or function, acting on the host epithelial and immunological responses [18], reducing intestinal inflammation and improving intestinal functions at clinical and biochemical levels when they are altered by an antimicrobial therapy [19–21].

*Clostridium butyricum* MIYAIRI 588 (CBM 588) is one probiotic bacterium used in antidiarrheal medicine in Japan. Our previous study revealed the impact of CLDM and CBM 588 on mice gut microbiome based on 16S rRNA sequencing and metagenomics analysis [22]. However, the impact of CLDM and CBM 588 on gut metabolic alterations has not been fully elucidated. To reveal the impact on the metabolic functional profiles of the gut microbiome, we performed Phylogenetic Investigation of Communities by Reconstruction of Unobserved States (PICRUSt) analysis to predict the relative abundance of metabolic pathways.

## 2. Material and methods

### 2.1. Medicine

CBM 588 bacterial powder was used for all *in vivo* experiments. It was composed of  $2.2 \times 10^{10}$  cfu/g (Lot 61 GT; Miyarisan Pharmaceutical Co., Ltd.). CLDM for injection was purchased from Pfizer Japan Inc. Immediately prior to each *in vivo* experiment, CBM 588 powder was weighed and reconstituted with sterile water. CLDM was further diluted in appropriate diluents to achieve the desired concentration.

### 2.2. Animals and housing

Specific-pathogen-free female ICR mice (9–10 weeks) weighing approximately 30 g were obtained from Charles River Laboratories Japan Inc. and utilized throughout the experiments. The animals were maintained and utilized in accordance with National Research Council recommendations and were provided food and water *ad libitum*. The study was reviewed and approved by the ethics committee of the Aichi Medical University (2018–100).

### 2.3. Method of the administration

Twenty female ICR mice were divided into the following four treatment groups, each consisting of 5 mice: control group, CLDM-treated group, CBM 588-treated group, and CBM 588 + CLDM-treated group (combination). CBM 588 was administered by oral gavage at a concentration of 500 mg/kg/day ( $3.4 \times 10^8$  cfu/kg/day). CLDM was also administered by oral gavage at a concentration of 40 mg/kg/day. CBM 588 powder was dissolved in sterilized water, mixed, and orally administered to mice using a sonde (0.2 mL for each mouse). For the treated group, CBM 588 and CLDM were dissolved in sterilized water separately and orally administered to mice twice a day, at 10 a.m. and 4 p.m., separately, using 1/2 dose every time for 4 days. For control group, sterilized water (0.2 mL) was orally administered to mice using a sonde at twice a day (at 10 a.m. and 4 p.m.).

### 2.4. Sampling

Before adding the treatment (day 0), the 2nd and 4th day of treatment, the 2nd (day 6), 4th (day 8), 6th (day 10), 8th (day 12),

10th (day 14), 12th (day 16), and 14th (day 18) day after termination were the examining days. At those selected days, at least 0.3 g feces were collected and transferred to 0.45 mL of transport medium.

### 2.5. DNA extraction

To characterize the microbiome composition in the colon, fecal samples from each mouse were analyzed by sequencing the 16S rRNA gene V3–V4 regions. DNA extraction and sequencing of 16S rRNA encoding gene amplicons were conducted as previously described [23].

### 2.6. Gut microbiome analysis

Meta 16S rRNA gene sequencing polymerase chain reaction (PCR) was performed as previously described [22]. As for the sequence analysis pipeline, the 16S rRNA sequence data generated by the MiSeq sequencer (Illumina) were processed by quantitative insights into microbial ecology (QIIME v1.9.1) pipeline [24,25]. Sequences with an average quality value of <20 were filtered out. Chimeric sequences were removed using USEARCH [26]. Sequences were clustered into operational taxonomic units (OTUs) based on 97% sequence similarity at the species level using UCLUST [26] against Greengenes database 13\_8 [27]. A representative sequence for each OTU was aligned with PyNAST [24]. Bacterial taxonomy was assigned using UCLUST. Genomic DNA from 20 Strain Even Mix Genomic Material (ATCC<sup>®</sup> MSA-1002<sup>™</sup>) was used to evaluate data analysis procedures. The relative abundances of the fecal metagenome categories were calculated and graphed using Microsoft Excel software (Microsoft).

### 2.7. Predictive functional profiling of gut microbial communities

To gain more insight into the metagenomics-based function of the microbiome in each mice group, the Phylogenetic Investigation of Communities by Reconstruction of Unobserved States (PICRUSt) v1.1.1 was used [28]. PICRUSt was used to obtain relative Kyoto Encyclopedia of Genes and Genomes (KEGG) pathway abundance information derived from metagenomics data [28]. The predicted data were collapsed into hierarchical categories (KEGG-Level-2 and 3), and the relative abundances of the gut metabolic functions were calculated and graphed using Microsoft Excel software. We only focused on level 2 and 3 to investigate the impact of CLDM and CBM 588 treatments on gut microbial functions.

### 2.8. Statistical analysis

*P*-value for a significant difference between the mean relative abundances of each group was recognized as  $p < 0.05$ . Data analyses were performed by using the one-way analysis of variance (ANOVA) to test homogeneity of variances.

## 3. Results

### 3.1. Gut microbiome

Changes to the murine gut microbiome at phylum level during the study period are shown in Fig. 1. Bar graphs depict the mean percent abundances of bacteria at the phylum level. At the phylum level, intestinal flora mainly consisted of Firmicutes phylum and Bacteroidetes phylum in the control and CBM 588-treated group. CLDM treatment in mice resulted in a dramatic increase in the Firmicutes phylum compared to the other groups from the beginning of the treatment. The Proteobacteria phylum also dramatically increased at day 2. These compositions began back to similar

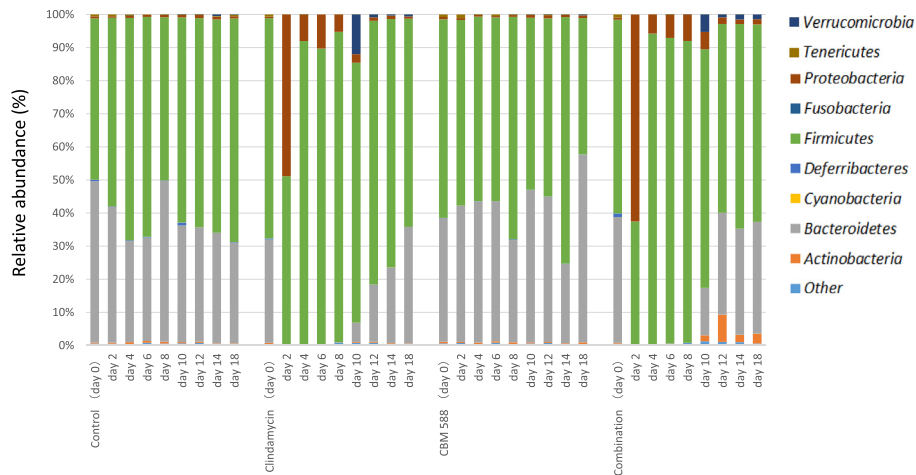


**Fig. 1.** Changes to the mice gut microbiome. Bar graphs depict the mean relative abundances (%) of bacterial phyla of the control group (Control), clindamycin-treated group (Clindamycin), CBM 588-treated group (CBM 588), and CBM 588 + clindamycin-treated group (Combination).

composition to the control group 6–8 days after the treatment was stopped. In the CBM 588 + CLDM-treated group, the transition of gut microbiome was very similar to that observed in the CLDM-treated group. However, the Actinobacteria phylum (mainly *Bifidobacterium*) increased only in the CBM 588 + CLDM-treated group after the 6th day of treatment termination (day 10).

### 3.2. Predictive functional profiling of gut microbial communities

The overall metabolic functions such as carbohydrate, amino acid, lipid metabolisms (KEGG-Level-2 categories) were largely conserved across the treatment groups (Fig. 2). The gut microbiome showed higher relative abundance of carbohydrate metabolism compared to the other metabolic pathways. The relative abundance of carbohydrate metabolism in the CLDM-treated groups (including CBM 588 + CLDM-treated group) showed a downward trend during the treatment period. However, they returned to equal levels or increased to higher levels than that of the control group after treatment period. The relative abundance of lipid and amino acid metabolism was relatively stable in all groups.

### 3.3. Investigations of carbohydrate metabolism

Investigations of the KEGG-Level-3 subcategories from carbohydrate metabolism showed in Fig. 3. The relative abundance of starch and sucrose metabolism (E) in CLDM-treated group decreased during the treatment period compared to the control group ( $p < 0.05$ ) (Fig. 3). However, the relative abundance of pyruvate metabolism (F) and butyric acid metabolism (D) in the CLDM-treated group increased compared to the control group ( $p < 0.05$ ). After CLDM treatment, glycolysis/gluconeogenesis (A), pentose phosphate pathway (B), fructose and mannose metabolism (C), starch and sucrose metabolism (E), pyruvate metabolism (F), and butyric acid metabolism (D) in the CLDM-treated group increased compared to the control group ( $p < 0.05$ ). The relative abundance of some metabolic pathways in the CBM 588 + CLDM-treated group showed a trend similar to that of the CLDM-treated group (Fig. 3 and Supplemental data 1). However, the CBM 588 + CLDM-treated group showed higher relative abundance of starch and sucrose metabolism (E) (day 12:  $1.2726 \pm 0.0812$  vs.  $1.1139 \pm 0.0171$ ,  $p = 0.0027$ ) than those in the CLDM-treated group.

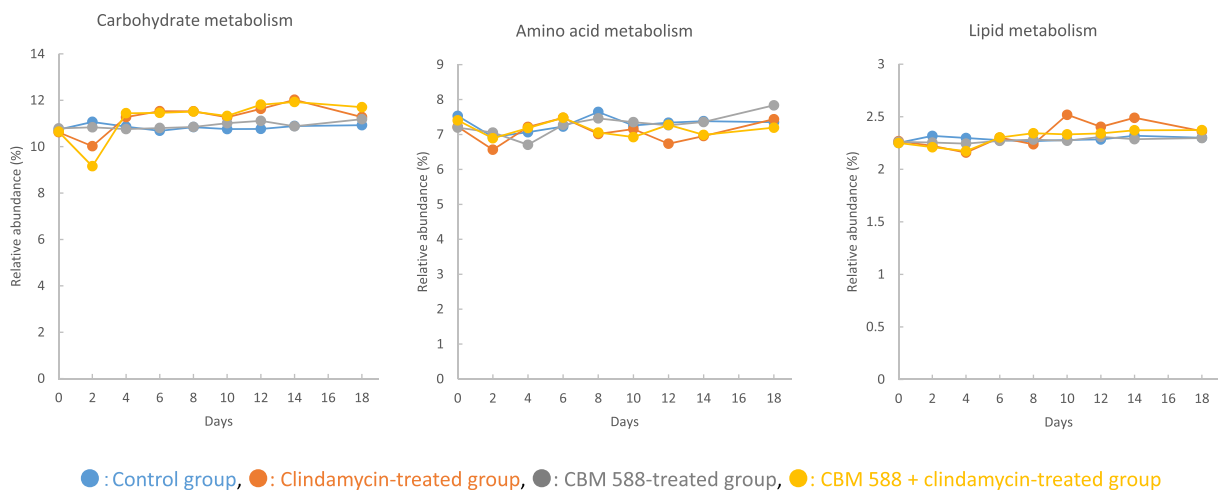


**Fig. 2.** Changes to the mice gut metabolic functions. Graphs depict the relative abundances (%) of metabolic pathways of carbohydrate, amino acid, lipid, metabolism (Kyoto Encyclopedia of Genes and Genomes (KEGG)-Level-2 categories).

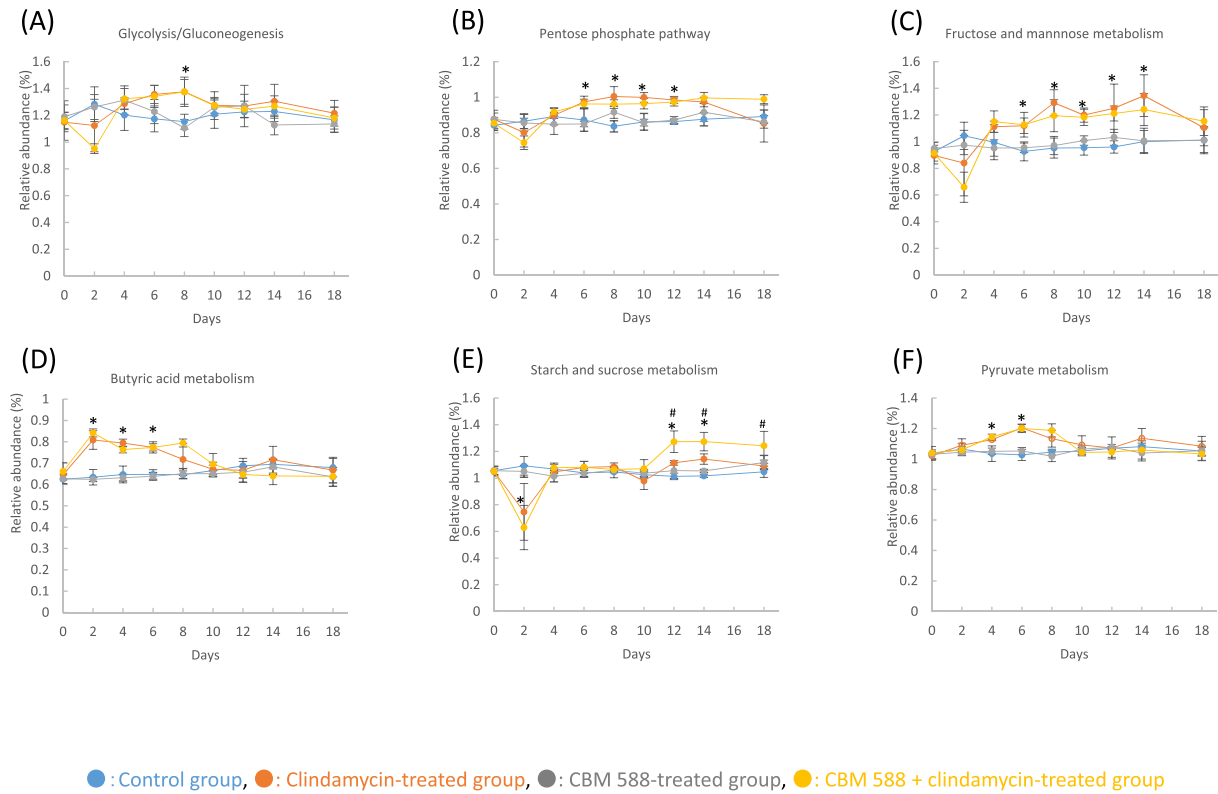


**Fig. 3. Changes to the mice gut carbohydrate metabolism.** Graphs depict the relative abundances (%) of metabolic pathways of carbohydrate metabolism (Kyoto Encyclopedia of Genes and Genomes (KEGG)-Level-3 subcategories). \*:  $p < 0.05$  when compared relative abundances (%) in the clindamycin-treated group to the control group. #:  $p < 0.05$  when compared relative abundances (%) in the CBM 588 + clindamycin-treated group to the clindamycin-treated group.

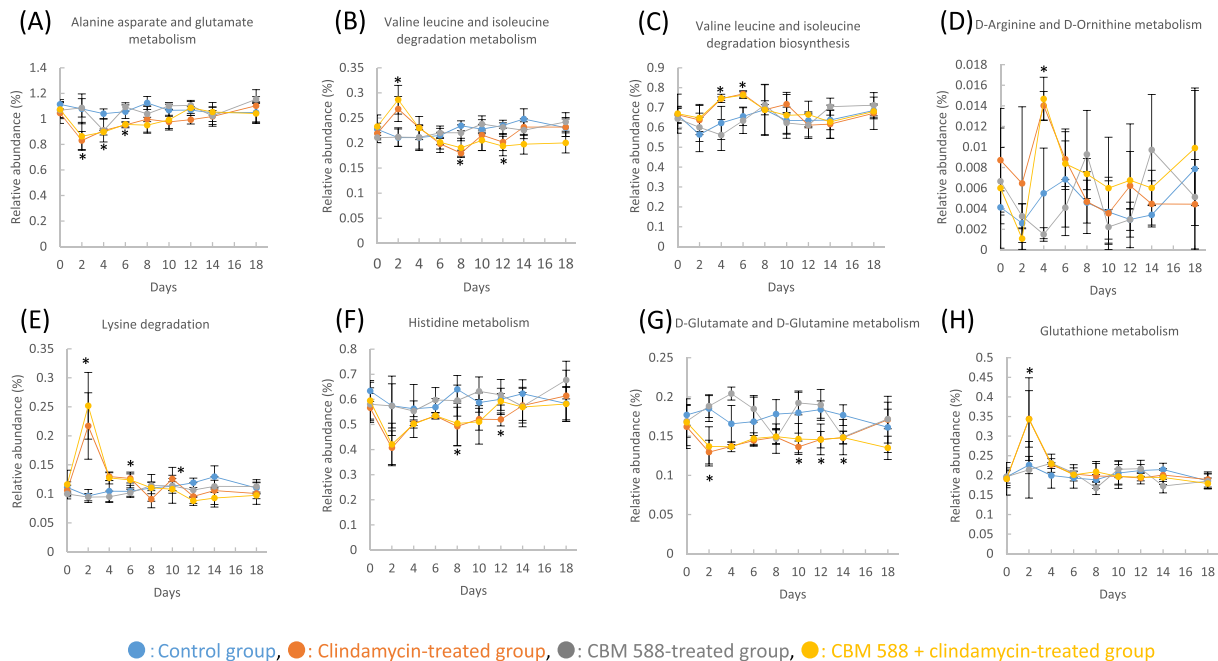


**Fig. 4. Changes to the mice gut amino acid metabolism.** Graphs depict the relative abundances (%) of metabolic pathways of amino acid metabolism (Kyoto Encyclopedia of Genes and Genomes (KEGG)-Level-3 subcategories). \*:  $p < 0.05$  when compared relative abundances (%) in the clindamycin-treated group to the control group. #:  $p < 0.05$  when compared relative abundances (%) in the CBM 588 + clindamycin-treated group to the clindamycin-treated group.

### 3.4. Investigations of amino acid metabolism

Investigations of the KEGG-Level-3 subcategories from amino acid metabolism showed in Fig. 5. The relative abundance of

alanine aspartate and glutamate metabolism (A), D-glutamate and D-glutamine metabolism (G) in the CLDM-treated group decreased during the treatment period compared to the control group ( $p < 0.05$ ) (Fig. 4). However, the relative abundance of valine leucine

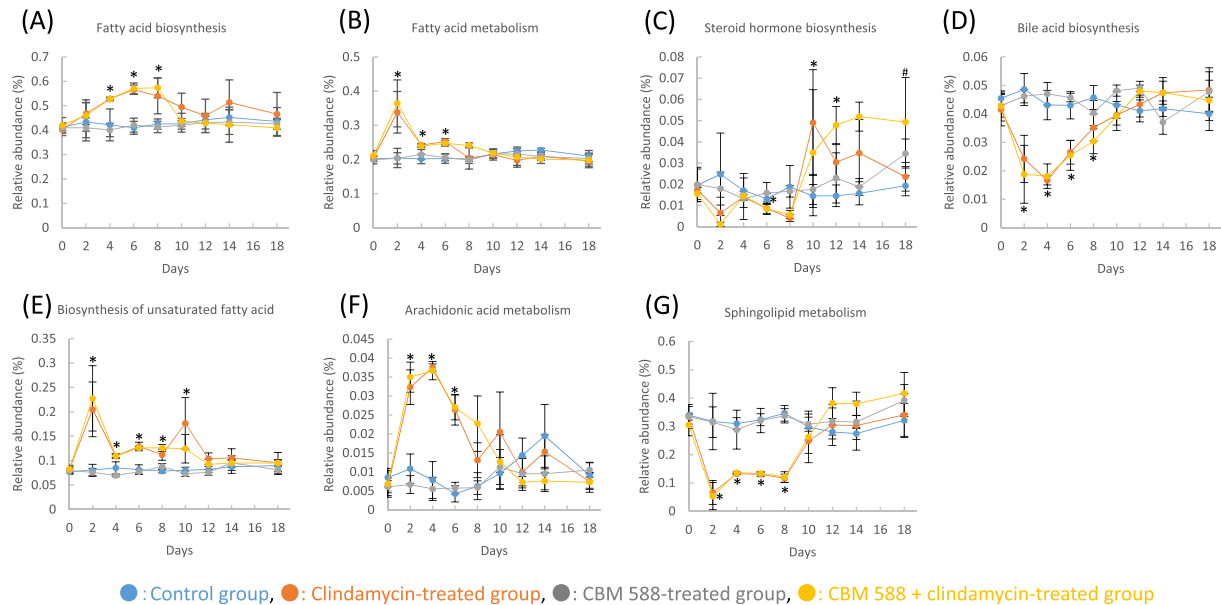


**Fig. 5.** Changes to the mice gut lipid metabolism. Graphs depict the relative abundances (%) of metabolic pathways of lipid metabolism (Kyoto Encyclopedia of Genes and Genomes (KEGG)-Level-3 subcategories). \*:  $p < 0.05$  when compared relative abundances (%) in the clindamycin-treated group to the control group. #:  $p < 0.05$  when compared relative abundances (%) in the CBM 588 + clindamycin-treated group to the clindamycin-treated group.

and isoleucine degradation metabolism (B), valine leucine and isoleucine degradation biosynthesis (C), lysin degradation (E), D-arginine and D-ornithine metabolism (D), and glutathione metabolism (H) increased compared to the control group ( $p < 0.05$ ). After CLDM treatment, the relative abundance of valine leucine and isoleucine degradation biosynthesis (C), lysine degradation (E), and metabolism in the CLDM-treated group increased compared to the control group, while the valine leucine and isoleucine degradation metabolism (B), lysine degradation (E), histidine metabolism (F) decreased ( $p < 0.05$ ). The relative abundance of most metabolic pathways in the CBM 588 + CLDM-treated group showed a trend similar to that in the CLDM-treated group (Fig. 4 and Supplemental data 2). There was no significant difference in the relative abundance profiles between the CBM 588 + CLDM-treated group and the CLDM-treated group.

### 3.5. Investigations of lipid metabolism

Investigations of the KEGG-Level-3 subcategories from fatty acid metabolism showed in Fig. 5. The relative abundance of bile acid biosynthesis (D) and sphingolipid metabolism (G) in the CLDM-treated group decreased during the treatment period compared to the control group ( $p < 0.05$ ) (Fig. 5). However, the relative abundance of fatty acid biosynthesis (A), fatty acid metabolism (B), biosynthesis of unsaturated fatty acid (E) and arachidonic acid metabolism (F) in the CLDM-treated group increased compared to the control group ( $p < 0.05$ ). After CLDM treatment, the relative abundance of steroid hormone biosynthesis (C), and unsaturated fatty acid biosynthesis (E), fatty acid metabolism (B), and arachidonic acid metabolism (F) in the CLDM-treated group increased compared to the control group ( $p < 0.05$ ), while bile acid biosynthesis (D) and sphingolipid metabolism (G) decreased ( $p < 0.05$ ). The relative abundance of most metabolic pathways in the CBM 588 + CLDM-treated group showed a trend similar to the CLDM-treated group (Fig. 5 and Supplemental data 3). However, the CBM 588 + CLDM-treated group showed higher relative abundance in steroid hormone

biosynthesis (C) (day 18:  $0.0493 \pm 0.0210$  vs.  $0.0236 \pm 0.0068$ ,  $p = 0.0311$ ) than that in the CLDM-treated group.

## 4. Discussion

The tissue microenvironment can influence nutrient availability, affecting the gut microbiome, because intestinal bacteria compete for the limited supply of nutrients within the intestine. In this study, the overall metabolic function (KEGG-Level-2 categories) was largely conserved in each treatment group, even with widespread differences in gut bacteria composition (Figs. 1 and 2). However, the activities of detailed metabolic pathways (KEGG-Level-3 subcategories) showed considerable variations.

By using PICRUSt, a bioinformatics program with considerable efficacy in the predictions of metabolic functions of microbial communities, we were able to predict that the activity of some metabolic pathways decreased upon CLDM therapy. At the same time, the other metabolic pathway worked in a complementary manner to keep fixed amount of energy production. Especially, some metabolic changes were seemed likely to keep the carbohydrate metabolite activities.

In our previous study, only the CLDM-treated group showed abnormal colon mucosa after CLDM treatment [22]. In this group, histologic examination showed superficial epithelial necrosis and presence of inflammatory cells. On the other hand, control, CBM 588, the CBM 588 + CLDM-treated group showed histological normal colon mucosa. Considering the increased relative abundance of glycolysis/gluconeogenesis, pentose phosphate pathway, fructose and mannose, starch and sucrose, and pyruvate metabolism in the gut tissue after CLDM treatment (Fig. 3), we may speculate that inflamed tissue provides less supply of glucose [29]. Thus, gut microbiome shifted to enhance pentose phosphate pathway, fructose and mannose metabolism, starch and sucrose metabolism to produce glucose for carbohydrate metabolism. Additionally, the increased relative abundance of butyric acid metabolism in the CLDM-treated and CBM 588 + CLDM-treated

group indicated that gut microbiome function shifted toward the repair of superficial epithelial necrosis on colon mucosa [30].

Moreover, especially in starch and sucrose metabolism, CBM 588 + CLDM-treated group showed higher relative abundance compared to the CLDM-treated group (Fig. 3). Considering the increased abundance of *Bifidobacterium*, limited species can use starch and sucrose as energy source in the gut microbiome, only in the CBM 588 + CLDM-treated group, as our previous study revealed [22], it appears that CBM 588 indirectly enhanced starch and sucrose metabolism to produce glucose with the increase of *Bifidobacterium*. And the microbiome change may contribute to attenuate colon epithelial damages.

In amino acid metabolism, the reductions of relative function of histidine metabolism, D-glutamate and D-glutamine metabolism and alanine aspartate and glutamate metabolism in the CLDM-treated and CBM 588 + CLDM-treated group were admitted (Fig. 4). Dietary glutamate is absorbed from the gut by an active transport system into mucosal cells where it is metabolized as a significant energy [5]. Hence, these changes may lead to a shortage of metabolic fuel in intestine mucosa. Besides, the increase in relative function of valine leucine and isoleucine degradation, lysine degradation, D-arginine and D-ornithine metabolism, and glutathione metabolism in the CLDM-treated and CBM 588 + CLDM-treated group indicated that gut microbiome function shifted toward the enhance of tricarboxylic acid (TCA) cycle accompanied by the activation of urea cycle and pyruvate production, because utilization of arginine as a carbon source entailed deamination of glutamate to  $\alpha$ -ketoglutarate, which was then channeled into the TCA cycle [31].

In lipid metabolism, the increase in relative function of fatty acid biosynthesis and fatty acid biosynthesis metabolism (Fig. 5), arachidonic acid metabolism, and steroid hormone and unsaturated fatty acid biosynthesis in the CLDM-treated and CBM 588 + CLDM-treated group indicated that gut microbiome function shifted toward the production of some kinds of prostaglandins to react the inflammation of colon mucosa [32].

Interestingly, the mucus layer in the intestinal tract is an important barrier to luminal bacteria and a major substrate and adhesion component for bacteria living in this microenvironment. Alterations of the mucus layer due to antimicrobials can lead to breaches of the epithelial barrier by specific bacteria, resulting in immune responses that can result in chronic inflammation [22]. Changes in the quantity and quality of this mucus layer influence the constituency of attached microbial populations. Since mucin is an important source of carbohydrates for the commensal bacteria, gut mucosal microbiome in inflamed regions can shift toward bacteria that can metabolize pentose, starch and sucrose, and amino acids to keep fixed amount of energy production with the activation of carbohydrate metabolism [33].

Our study suggested that CLDM reduced the activities of carbohydrate metabolism. However, gut amino acid metabolism shifted to enhance TCA cycle due to activation of urea cycle and pyruvate production. Gut fatty acid metabolism also shifted to produce some kinds of prostaglandins to attenuate the inflammation of colon mucosa. Additionally, CBM 588 enhanced starch and sucrose metabolism to produce glucose due to the increase of *Bifidobacterium* in the CBM 588 + CLDM-treated group. As results, these functions of CBM 588 resulted beneficial for the protection of colon mucosa [22].

However, our study has some limitations. Microbiome in mice fecal sample showed some differences at the family, genus, and species level between the gut microbiome of mice and humans, while this microbiome showed similar compositions as human at phyla level [34]. Hence, the properties of CBM 588 should be investigated in carefully planned and controlled human studies in the future.

## 5. Conclusion

This is the first report showing that gut metabolic function can be altered by CLDM and CBM 588. We found that the alteration in gut metabolic function was more considerably in CLDM-treated mice than non-treated mice. Additionally, this study provides new insight into the CBM 588 function. CBM 588 contributed to increase carbohydrate metabolism to repair mucosal layer of the gastrointestinal tract. These results support the hypothesis that CBM 588 treatment modulates gut microbiome under dysbiosis conditions due to antimicrobials. Further metagenomics analysis would help substantiate the metabolic attributes of the gut microbiome in benefitting health and digestive physiology.

## Conflicts of interest

H. Mikamo has received speaker honoraria and/or grants and/or donations and/or consultant fees from Astellas Pharma Inc., Bayer Yakuhin Co., Ltd., Daiichi Sankyo Co., Ltd., Kyorin Pharmaceutical Co., Ltd., Meiji Seika Pharma Co., Ltd., MSD K.K., Pfizer Japan Inc., Shionogi & Co., Ltd., Sumitomo Dainippon Pharma Co., Ltd., Taisho Toyama Pharmaceutical Co., Ltd., Toyama Chemical Co., Ltd. and Taisho Pharmaceutical Co., Ltd.

## Acknowledgments

This work was mainly funded by Miyarisan Pharmaceutical Co., Ltd. They provided the CBM 588 bacterial powder. We would like to thank Editage ([www.editage.jp](http://www.editage.jp)) for English language editing.

## Appendix A. Supplementary data

Supplementary data to this article can be found online at <https://doi.org/10.1016/j.jiac.2019.02.008>.

## References

- [1] Human Microbiome Project Consortium. Structure, function and diversity of the healthy human microbiome. *Nature* 2012;486:207–14.
- [2] Qin J, Li R, Raes J, Arumugam M, Burgdorf KS, Manichanh C, et al. A human gut microbial gene catalogue established by metagenomic sequencing. *Nature* 2010;464:59–65.
- [3] Frank DN, St Amand AL, Feldman RA, Boedeker EC, Harpaz N, Pace NR. Molecular-phylogenetic characterization of microbial community imbalances in human inflammatory bowel diseases. *Proc Natl Acad Sci USA* 2007;104:13780–5.
- [4] Manichanh C, Rigottier-Gois L, Bonnaud E, Gloux K, Pelletier E, Frangeul L, et al. Reduced diversity of faecal microbiota in Crohn's disease revealed by a metagenomics approach. *Gut* 2006;55:205–11.
- [5] Morgan XC, Tickle TL, Sokol H, Gevers D, Devaney KL, Ward DV, et al. Dysfunction of the intestinal microbiome in inflammatory bowel disease and treatment. *Genome Biol* 2012;13:R79.
- [6] Fite A, Macfarlane S, Furrer E, Bahrami B, Cummings JH, Steinke DT, et al. Longitudinal analyses of gut mucosal microbiotas in ulcerative colitis in relation to patient age and disease severity and duration. *J Clin Microbiol* 2013;51:849–56.
- [7] Honda K, Littman DR. The microbiome in infectious disease and inflammation. *Annu Rev Immunol* 2012;30:759–95.
- [8] Sokol H, Lay C, Seksik P, Tannock GW. Analysis of bacterial bowel communities of IBD patients: what has it revealed? *Inflamm Bowel Dis* 2008;14:858–67.
- [9] Ott SJ, Musfeldt M, Wenderoth DF, Hampe J, Brant O, Fölsch UR, et al. Reduction in diversity of the colonic mucosa associated bacterial microflora in patients with active inflammatory bowel disease. *Gut* 2004;53:685–93.
- [10] Swidsinski A, Ladhoff A, Pernthaler A, Swidsinski S, Loening-Baucke V, Ortner M, et al. Mucosal flora in inflammatory bowel disease. *Gastroenterology* 2002;122:44–54.
- [11] Dethlefsen L, Huse S, Sogin ML, Relman DA. The pervasive effects of an antibiotic on the human gut microbiota, as revealed by deep 16S rRNA sequencing. *PLoS Biol* 2008;6:e280.
- [12] Dethlefsen L, Relman DA. Incomplete recovery and individualized responses of the human distal gut microbiota to repeated antibiotic perturbation. *Proc Natl Acad Sci USA* 2011;108:4554–61.

- [13] Rashid M, Zaura E, Buijs MJ, Keijser BJJ, Crielaard W, Nord CE, et al. Determining the long-term effect of antibiotic administration on the human normal intestinal microbiota using culture and pyrosequencing methods. *Clin Infect Dis* 2015;60:S77–84.
- [14] Greenblum S, Turnbaugh PJ, Borenstein E. Metagenomic systems biology of the human gut microbiome reveals topological shifts associated with obesity and inflammatory bowel disease. *Proc Natl Acad Sci USA* 2012;109:594–9.
- [15] Zaura E, Brandt BW, Teixeira de Mattos MJ, Buijs MJ, Caspers MP, Rashid MU, et al. Same exposure but two radically different responses to antibiotics: resilience of the salivary microbiome versus long-term microbial shifts in feces. *mBio* 2015;6. e01693-15.
- [16] Guay D. Update on clindamycin in the management of bacterial, fungal and protozoal infections. *Expert Opin Pharmacother* 2007;8:2401–44.
- [17] Food and Agriculture Organisation of the United Nations and WHO Working Group. Guidelines for the evaluation of probiotics in food. Geneva, Switzerland: FAO/WHO; 2002.
- [18] Rogers GB, Carroll MP, Hoffman LR, Walker AW, Fine DA, Bruce KD. Comparing the microbiota of the cystic fibrosis lung and human gut. *Gut Microb* 2010;1:85–93.
- [19] Whelan K, Quigley EMM. Probiotics in the management of irritable bowel syndrome and inflammatory bowel disease. *Curr Opin Gastroenterol* 2013;29:184–9.
- [20] Gollwitzer ES, Marsland BJ. Microbiota abnormalities in inflammatory airway diseases—potential for therapy. *Pharmacol Ther* 2014;141:32–9.
- [21] Vernocchi P, Del Chierico F, Fiocchi AG, El Hachem M, Dallapiccola B, Rossi P, et al. Understanding probiotics' role in allergic children: the clue of gut microbiota profiling. *Curr Opin Allergy Clin Immunol* 2015;15:495–503.
- [22] Hagihara M, Yamashita R, Matsumoto A, Mori T, Kuroki Y, Kudo H, et al. The impact of *Clostridium butyricum* MIYAIRI 588 on the murine gut microbiome and colonic tissue. *Anaerobe* 2018;54:8–18.
- [23] Hayashi A, Mikami Y, Miyamoto K, Kamada N, Sato T, Mizuno S, et al. Intestinal dysbiosis and biotin deprivation induce alopecia through overgrowth of *Lactobacillus murinus* in mice. *Cell Rep* 2017;20:1513–24.
- [24] Caporaso JG, Bittinger K, Bushman FD, DeSantis TZ, Andersen GL, Knight R. PyNAST: a flexible tool for aligning sequences to a template alignment. *Bioinformatics* 2010;26:266–7.
- [25] Caporaso JG, Kuczynski J, Stombaugh J, Bittinger K, Bushman FD, Costello EK, et al. QIIME allows analysis of high-throughput community sequencing data. *Nat Methods* 2010;7:335–6.
- [26] Edgar RC. Search and clustering orders of magnitude faster than BLAST. *Bioinformatics* 2010;26:2460–1.
- [27] DeSantis TZ, Hugenholtz P, Larsen N, Rojas M, Brodie EL, Keller K, et al. Green genes, a chimera-checked 16S rRNA gene database and workbench compatible with ARB. *Appl Environ Microbiol* 2006;72:5069–72.
- [28] Langille MG, Zaneveld J, Caporaso JG, McDonald D, Knights D, Reyes JA, et al. Predictive functional profiling of microbial communities using 16S rRNA marker gene sequences. *Nat Biotechnol* 2013;31:814–21.
- [29] Davenport M, Poles J, Leung JM, Wolff MJ, Abidi WM, Ullman T, et al. Metabolic alterations to the mucosal microbiota in inflammatory bowel disease. *Inflamm Bowel Dis* 2014;20:723–31.
- [30] Brown CT, Davis-Richardson AG, Giongo A, Gano KA, Crabb DB, Mukherjee N, et al. Gut microbiome metagenomics analysis suggests a functional model for the development of autoimmunity for type 1 diabetes. *PLoS One* 2011; e25792.
- [31] Hashim S, Kwon DH, Abdelal A, Lu CD. The arginine regulatory protein mediates repression by arginine of the operons encoding glutamate synthase and anabolic glutamate dehydrogenase in *Pseudomonas aeruginosa*. *J Bacteriol* 2004;186:3848–54.
- [32] Srivastava KC, Awasthi KK, Lindgård P, Tiwari KP. Effect of some saturated and unsaturated fatty acids on prostaglandin biosynthesis in washed human blood platelets from (1-14 C) arachidonic acid. *Prostaglandins Leukot Med* 1982;8:219–37.
- [33] Kamada N, Chen GY, Inohara N, Núñez G. Control of pathogens and pathobionts by the gut microbiota. *Nat Immunol* 2013;14:685–90.
- [34] Bartlett JG, Chang TW, Gurwith M, Gorbach SL, Onderdonk AB. Antibiotic-associated pseudomembranous colitis due to toxin-producing clostridia. *N Engl J Med* 1978;298:531–4.